Influence of voids on the engineering constants of paper

Part 1: Continuum modeling

Lakshmikanthan Subramanian and Leif A. Carlsson

ABSTRACT: The influence of voids on the engineering elastic constants of paper is investigated in two parts. Part 1 describes a continuum micromechanical model that generates in-plane elastic constants and moisture-expansion coefficients of void-free papers composed of chemical pulp fibers. Predictions from the model are compared with existing experimental data from the literature. The modeling of voids, correction of baseline properties for voids, and further experimental comparisons are reported in the second part of the study.

KEYWORDS: Bibliographies, chemical pulps, coefficients, elasticity, engineering, equations, fibers, hygroexpansivity, laminates, mechanical properties, models, voids.

Modeling of the heterogeneous structure of paper presents substantial obstacles because the sheet structure contains such a wide spectrum of void and fiber geometries, fiber orientations, and degrees of bonding. Accordingly, a range of idealized micromechanical theories have emerged since the early 1950s.

Steenberg *(1)* approached the viscoelastic response of paper by a phenomenological model based on an assemblage of springs and dashpots, but the first micromechanical model was developed by Cox *(2)*, who considered paper as a geometrical network of continuous fibers and derived the elastic properties of the sheet in terms of the axial modulus of the fibers. Many researchers (e.g., *3–7)* extended Cox's theory to incorporate various microscopic features of the network structure of paper, such as finite fiber length, bonds, etc. The network models should be most appropriate for low-density papers, where free fiber segments are clearly identifiable. At higher apparent sheet densities, the fibers attain a more closely packed configuration, and the sheet loses its network character. Nissan *(8)* considered paper as a hydrogen-bonded homogeneous solid and derived the elastic constants from a Morse function governing the elongation of hydrogen bonds. Continuum models based on a composite-materials approach have been developed by Salmen *et al. (9)* and Schulgasser and Page *(10)*, who treated paper as having a homogeneous structure composed of cell-wall material that is bonded together throughout the entire volume of the paper. Although such models provide insight into the mechanical response of paper, they can not readily be applied for quantitative predictions of elastic moduli, since the presence of voids in a material reduces the elastic stiffnesses *(11, 12)*.

We will describe the modeling of papers containing voids in two parts. Part 1 addresses the development of a continuum laminate model for predicting baseline elastic properties and hygroexpansion coefficients for papers without voids. Part 2 will discuss the influence of voids on the hygroelastic response of paper *(13)*.

Analysis

Laminate model

Laminate modeling of paper requires (a) determination of the elastic constants and coefficients of hygroexpansion of the constituent plies of the laminate and (b) specifi-

Subramanian, graduate student, and Carlsson, professor, are affiliated with the Dept. of Mechanical Engineering, Florida Atlantic University, Boca Raton, FL 33431.

1. Cell wall of a wood fiber. The middle lamella is composed of lignin; S_1, S_2, and S_3 represent the three layers of the secondary wall.

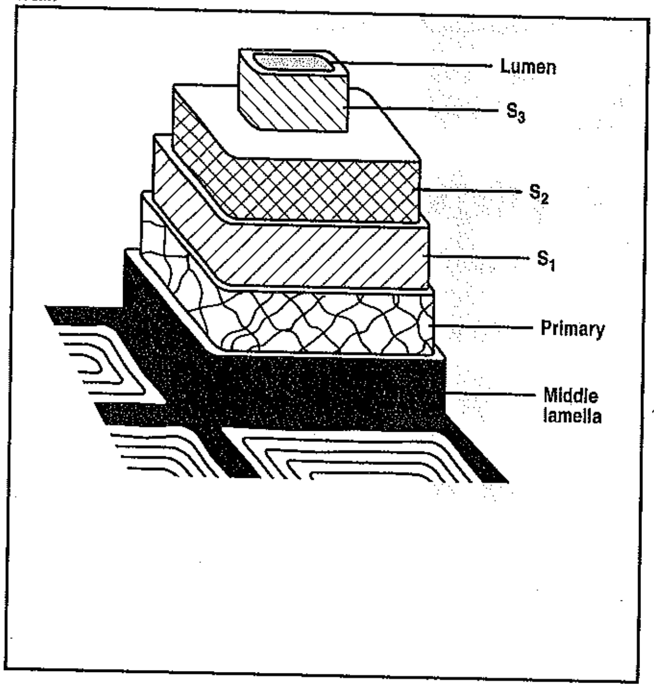

2. Laminate model of paper

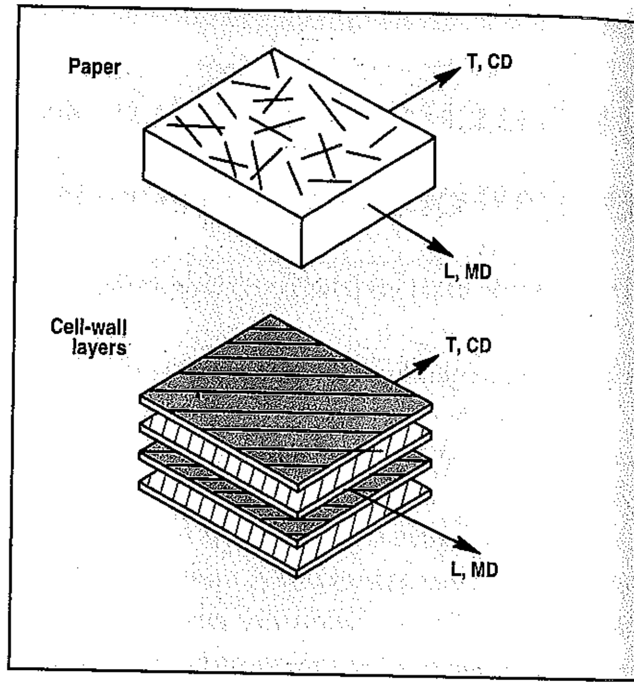

cation of the orientation of the plies with respect to the principal symmetry axes of the sheet. Summation of the contributions of each constituent ply provides the elastic and hygroex- pansional responses of the laminate.

The main structural unit of a sheet of paper is the wood fiber. Wood fibers resemble a hollow tube, as seen in **Fig. 1**, where the hollow region is called the lumen *(14)*. The cell wall consists of highly crystalline cellulose fibrils surrounded by amorphous hemicellulose and lignin. As shown in Fig. 1, the cell wall resembles a continuous, fiber-reinforced composite, with the cellulose reinforcements embedded within a matrix of hemicellulose and lignin *(15)*. Close examination of the fiber cell wall reveals that most of the lignin is located in the middle lamella between the fibers. The modulus of the wood fiber is largely governed by the S_2 layer and its fibril angle, α, which ranges between 10° and 30° *(16)*. In the modeling of paper, we will assume that the mechanical

I. Mechanical properties of cellulose and hemicellulose at dry condition

Cellulose	*Hemicellulose*
E_1 = 134 GPa	E = 8.0 GPa
E_2 = 27.2 GPa	
ν_{12} = 0.10	ν = 0.33
G_{12} = 4.4 GPa	
ρ = 1500 kg/m³	ρ = 1500 kg/m³

Based on data from the literature *(15, 20, 21)*

3. Orientation of a wood fiber in a paper sheet (θ) and of the fibrils within the wood fiber (α)

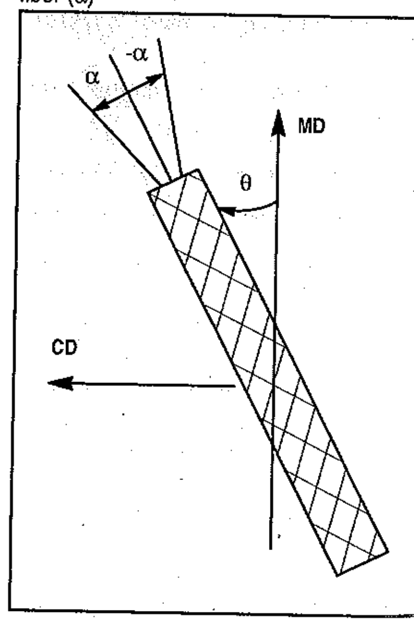

response of the wood fiber is entirely dominated by the S_2 layer.

The laminate model of paper thus considers the S_2 layer as the main structural unit and not the fiber *per se*. The orientation distribution for the fibrils is calculated from the fiber-orientation-distribution function, which is experimentally accessible. The fibril-orientation distribution is assumed to be symmetric with respect to the midplane, machine directio (MD), and cross-machine direction (CD) of the sheet. Based on laminated-plate theory *(17)*, it can be shown that the constitutive relation for such a sheet is

4. Effect of fibril orientation on the engineering elastic constants for sheets produced from bleached chemical pulp. **A:** longitudinal and transverse Young's moduli and the geometric mean modulus. **B:** in-plane shear modulus and Poisson's ratio.

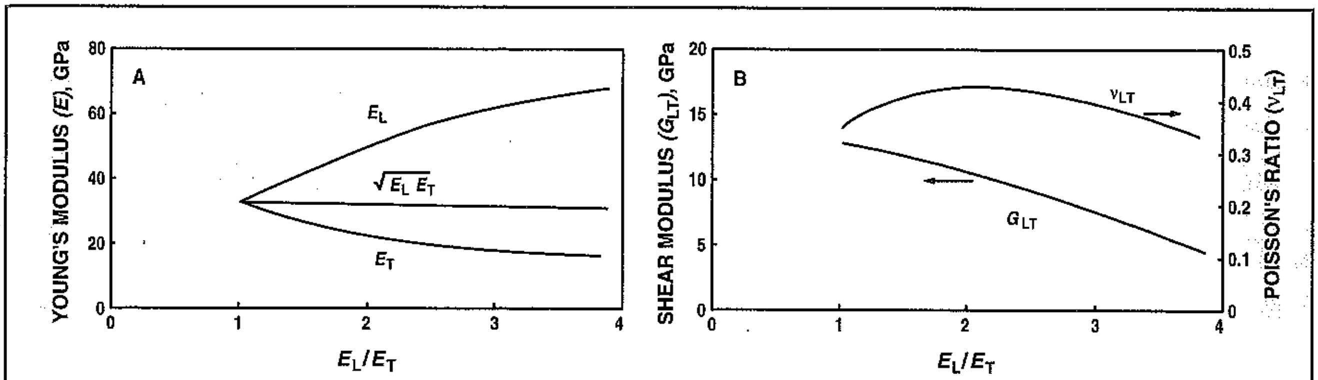

II. Elastic constants of paper calculated from laminate model at various fibril orientations at dry condition

$a_{C,1}$	$a_{C,2}$	E_L, GPa	E_T, GPa	G_{LT}, GPa	ν_{LT}	E_L/E_T
0	0	33.9	33.9	12.8	0.325	1.00
0.50	0.125	41.7	27.7	12.2	0.382	1.51
0.75	0.282	46.3	25.1	11.5	0.401	1.85
1.00	0.500	51.5	22.8	9.51	0.408	2.26
1.20	0.721	56.1	21.1	8.32	0.401	2.65
1.40	0.984	61.1	19.6	6.97	0.382	3.11
1.60	1.28	66.2	18.2	5.42	0.345	3.64

$$\begin{bmatrix} N_L \\ N_T \\ N_{LT} \end{bmatrix} + \begin{bmatrix} F_L \\ F_T \\ 0 \end{bmatrix} = \begin{bmatrix} A_{11} & A_{12} & 0 \\ A_{12} & A_{22} & 0 \\ 0 & 0 & A_{66} \end{bmatrix} \begin{bmatrix} \varepsilon_L \\ \varepsilon_T \\ \gamma_{LT} \end{bmatrix} \quad (1)$$

where the subscripts L and T refer to the longitudinal (MD) and transverse (CD) direction of the sheet, as seen in **Fig. 2**, and where

N_L, N_T, N_{LT} = mechanical stress resultants

F_L, F_T = effective hygroscopic forces

A_{ij} = extensional stiffnesses of the laminate *(17)* for $i, j = 1, 2, 6$

e_L, e_T = normal strains

g_{LT} = shear strain.

The effective hygroscopic forces, F_L and F_T, in a paper sheet of n plies are given by an equation presented in an earlier work *(18)*.

$$F_i = \Delta M \sum_{k=1}^{n} (\overline{Q}_{ij})_k (\overline{\beta}_j)_k h_k \qquad (2)$$

for

i, j = 1, 2, 6

where

F_1 = F_L, effective hygroscopic force in MD

F_2 = F_T, effective hygroscopic force in CD

ΔM = incremental moisture content

$\overline{Q}_{ij}$ = transformed reduced-ply stiffness *(17)*

$\overline{\beta}_j$ = transformed coefficient of hygroexpansion of a ply, defined as the moisture-induced strain (see Eqs. 4 and 5) divided by ΔM (see Eq. 6)

5. Calculated elastic moduli (left scale, continuous curves) and experimental values *(27)* (right scale, individual data points) as functions of humidity for sheets produced from chemical pulp

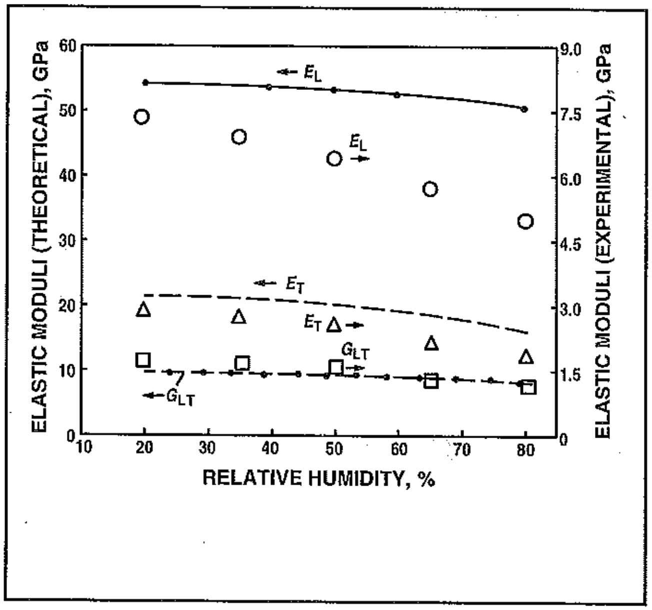

6. Calculated and experimental *(27)* Poisson's ratio as a function of humidity for sheets produced from chemical pulp

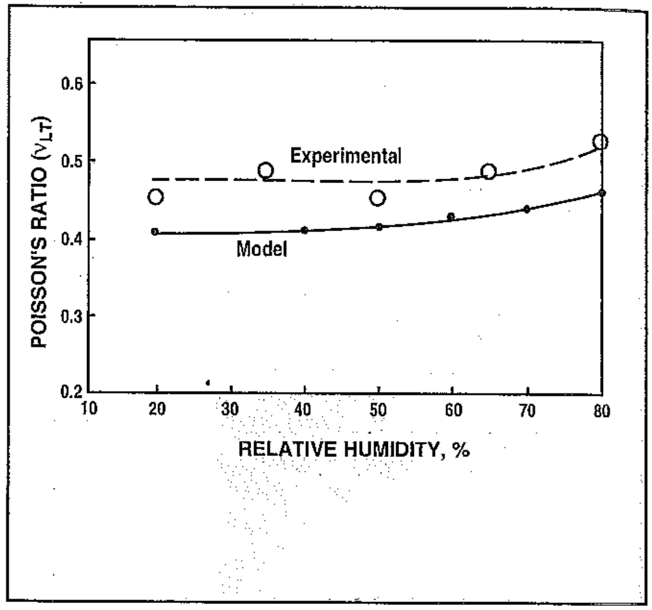

7. Calcu
humidity

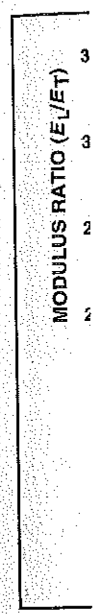

h_k = thickness of the kth ply in the laminate.

The engineering elastic constants are obtained from the laminate stiffnesses according to Salmen *et al. (9)*.

$$E_L = [A_{11} - (A_{12}^2/A_{22})]/h \quad (3a)$$

$$E_T = [A_{22} - (A_{12}^2/A_{11})]/h \quad (3b)$$

$$\nu_{LT} = A_{12}/A_{22} \quad (3c)$$

$$G_{LT} = A_{66}/h \quad (3d)$$

where

E_L, E_T = Young's moduli in the MD and CD, respectively

ν_{LT} = major Poisson's ratio

G_{LT} = in-plane shear modulus

h = total laminate thickness.

To calculate the coefficients of hygroexpansion for the laminate, Eq. 1—the constitutive relation—is considered, but with no external forces acting.

$$\begin{bmatrix} F_L \\ F_T \end{bmatrix} = \begin{bmatrix} A_{11} & A_{12} \\ A_{12} & A_{22} \end{bmatrix} \begin{bmatrix} e_L \\ e_T \end{bmatrix} \quad (4)$$

III. Elastic constants of paper calculated from laminate model at various relative humidities

Relative humidity, %	*E_L, GPa*	*E_T, GPa*	*G_{LT}, GPa*	*$[N]_{LT}$*	*E_L/E_T*
0	54.2	21.8	9.93	0.406	2.49
20	54.0	21.4	9.81	0.409	2.53
40	53.6	20.8	9.64	0.413	2.58
50	53.2	20.2	9.48	0.418	2.63
60	52.3	18.7	9.06	0.431	2.87
70	51.8	17.8	8.79	0.441	2.92
80	50.8	16.0	8.29	0.460	3.18

where

e_L, e_T = moisture-induced strains of the laminate in the MD and CD, respectively.

The moisture-induced strains of the laminate are obtained by inversion of Eq. 4.

$$e_L = (A_{22}F_L - A_{12}F_T)/(A_{11}A_{22} - A_{12}^2) \quad (5a)$$

$$e_T = (A_{11}F_T - A_{12}F_L)/(A_{11}A_{22} - A_{12}^2) \quad (5b)$$

The coefficients of hygroexpansion of the laminate are defined as

$$\beta_L = e_L/\Delta M \quad (6a)$$

$$\beta_T = e_T/\Delta M \quad (6b)$$

$$\beta_{LT} = 0 \quad (6c)$$

Fiber-orientation distribution

The orientation of the fibers in a paper sheet is a fundamental structural variable. If the orientation angle of a fiber with respect to the MD is taken as θ, as depicted in **Fig. 3**, the relative amount of fibers oriented in an angular region around θ can be represented by a probability-density function $f(\theta)$ *(10)*, where $f(\theta)d\theta$ is the fraction of fibers between the angles θ and θ + $d\theta$. The term $f(\theta)$ is commonly represented by a Fourier series *(10)*.

IV. Hyg
content

$a_{G,1}$
0
0.2
0.4
0.6
0.8
1.0
1.2

(

where

$a_{F,1}$ an

Since
sume
to the
terms
we w
to inc
and a

7. Calculated and experimental *(27)* modulus ratio as a function of humidity for sheets produced from chemical pulp

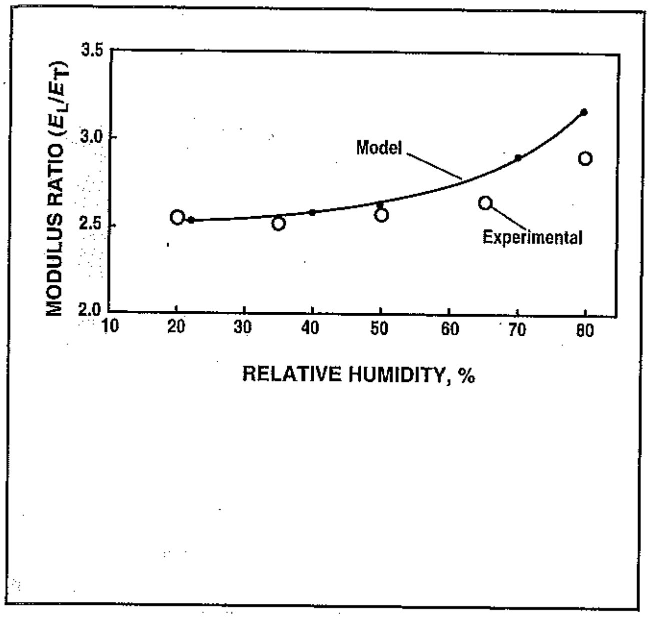

8. Effect of fibril orientation on the hygroexpansion ratio and geometric mean of hygroexpansion coefficients for sheets produced from bleached chemical pulp

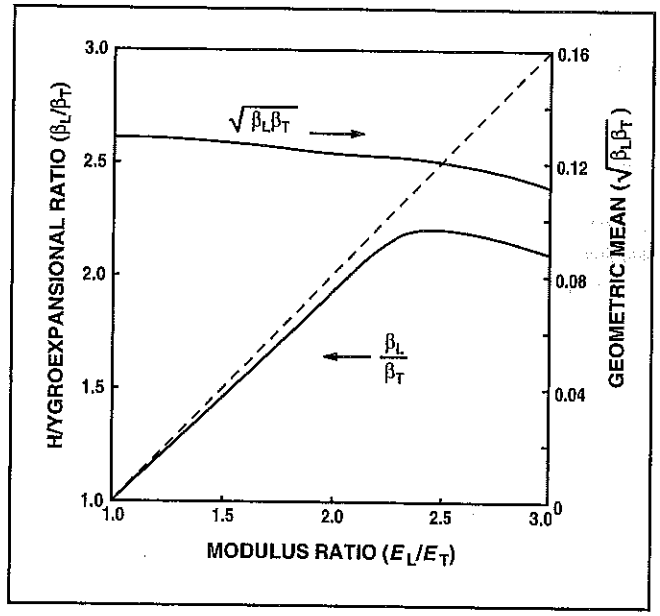

IV. Hygroexpansion coefficients calculated for isotropic and oriented sheets at 9% moisture content

$a_{C,1}$	$a_{C,2}$	β_L	β_T	β_T/β_L	E_L/E_T	$(\beta_L\beta_T)^{1/2}$
0	0	0.130	0.130	1.00	1.00	0.130
0.20	0.02	0.118	0.142	1.20	1.21	0.129
0.40	0.08	0.107	0.153	1.43	1.47	0.126
0.60	0.18	0.096	0.163	1.68	1.79	0.122
0.80	0.21	0.087	0.170	1.94	2.18	0.119
1.00	0.50	0.079	0.173	2.19	2.65	0.106
1.20	0.72	0.071	0.170	2.37	3.24	0.107

$$f(\theta) = (1 + a_{F,1}\cos 2\theta + a_{F,2}\cos 4\theta + a_{F,3}\cos 6\theta \ldots)/\pi \tag{7}$$

where

$a_{F,1}$ and $a_{F,2}$ = Fourier coefficients serving as fiber-orientation parameters, with the subscript "F" denoting fibers.

Since the distribution of fibers is assumed to be symmetric with respect to the MD and CD, only even cosine terms are included. In the following, we will truncate the Fourier series to include only two parameters, $a_{F,1}$ and $a_{F,2}$.

During stock preparation, the hollow lumen in the center of the fiber commonly collapses, and the fiber assumes a band-shaped structure *(6)*. For such a collapsed fiber of orientation θ, it is recognized that the fibrils will be oriented in the directions $\theta + \alpha$ and $\theta - \alpha$ with respect to the MD, as illustrated in Fig. 3. The orientation distribution of the fibrils is then modified according to Schulgasser and Page *(10)*.

$$f(\theta) = (1 + a_{C,1}\cos 2\theta + a_{C,2}\cos 4\theta)/\pi \tag{8}$$

where

$$a_{C,1} = a_{F,1}\cos 2\alpha \tag{9a}$$

$$a_{C,2} = a_{F,2}\cos 4\alpha \tag{9b}$$

where

$a_{C,1}$ and $a_{C,2}$ = Fourier coefficients serving as fibril-orientation parameters, with the subscript "C" denoting cellulose fibrils.

Notice that for isotropic sheets (random fiber orientation) $a_{C,1}$ and $a_{C,2}$ are zero, and $f(\theta) = 1/\pi$. We will assume here that the fibril-orientation parameters are related by the following approximate relation derived by Schulgasser *(19)*.

$$a_{C,2} \approx a_{C,1}^2/2 \tag{10}$$

Micromechanical modeling of the cell wall

As discussed previously, the main constituents of the wood fiber are cellulose, hemicellulose, and lignin. In this study, attention is limited to delignified fibers, but lignin will be incorporated in a future study. Cellulose fibrils are considered as transversely isotropic, while hemicellulose is considered as isotropic. **Table I** summarizes data on mechanical properties and densities of hemicellulose and cellulose at dry conditions.

These data are based on estimates for cellulose by Mark *(15)* and measurements on cellulose by Sakurada *et al. (20)* and on hemicellulose by Cousins *(21)*.

The cell wall is considered as a unidirectional composite, with the matrix composed of hemicellulose and the reinforcements consisting of cellulose fibrils of circular cross section, as illustrated in Figs. 1 and 2. For the delignified fibers considered herein, the volume fractions of the reinforcements and matrix are approximately: $V_f = 0.55$ and $V_m = 0.45$ *(9)*. Based on the Halpin–Tsai micromechanics estimates of composite properties *(22)* and the volume fractions and mechanical properties of the constituents listed in Table I, the following elastic constants of the cell wall (dry) are obtained: $E_1 = 77.3$ GPa, $E_2 = 15.8$ GPa, $G_{12} = 3.70$ GPa, and $\nu_{12} = 0.204$.

The elastic constants of the cell wall over a relative humidity range can be obtained by incorporating moisture softening of the hemicellulose matrix *(9, 23)*. The coefficients of hygroexpansion of the cell wall, β_1 and β_2, can be calculated from micromechanics *(24)* assuming a uniform moisture content, isotropic swelling, and volume additivity for the hemicellulose matrix *(9, 23)*. Micromechanical calculations indicate a slight dependence of β_1 and β_2 on moisture content *(23)*. At a moisture content of 9%, $\beta_1 = 0.024$ and $\beta_2 = 0.50$ *(23)*.

V. Hygroexpansion coefficients calculated from model and data of Salmen *et al. (9)**

Hygroexpansion coefficients	*Experimental*	*Salmen et al. (9) Laminate model*	*Present model*
Isotropic β	0.107	0.129	0.131
Oriented β_L	0.059	0.030	0.071
Oriented β_T	0.216	0.335	0.174
$(\beta_L\beta_T)^{1/2}$	0.113	0.100	0.111

*Experimental data for isotropic and oriented sheets made from bleached chemical pulp at 9% moisture content *(9)*

Results and discussion

Elastic constants

With knowledge of (a) the elastic constants and coefficients of hygroexpansion of the constituent cell-wall plies and (b) the fibril-orientation-distribution function, it is possible to establish the corresponding elastic constants of the laminate (paper) via the extensional stiffnesses A_{ij} calculated as outlined in the Appendix and Eq. 3.

The engineering constants of isotropic and oriented paper sheets (at dry condition) were calculated for various fibril-orientation parameters. Each set of orientation parameters corresponds to a unique set of elastic constants of the paper. A convenient way to express the anisotropy of the sheet is by the modulus ratio, E_L/E_T, and this convention is followed throughout this study.

Table II summarizes the calculated engineering constants at various fibril-orientation parameters. **Figure** 4 shows plots of the elastic constants vs. modulus ratio. As expected, Fig. 4A shows that E_L increases and E_T decreases with increased fibril orientation along the MD. The geometric mean of the moduli, $(E_LE_T)^{1/2}$, remains constant, independent of the fibril orientation. Htun and Fellers *(25)* experimentally demonstrated invariance of $(E_LE_T)^{1/2}$ for paper sheets of various fiber orientations. Figure 4B shows that the shear modulus, G_{LT}, decreases with increased fibril orientation, while the Poisson's ratio, ν_{LT}, goes through a maximum at about $E_L/E_T = 2.75$.

The literature contains very little consistent data on E_L, E_T, G_{LT}, and ν_{LT} for papers made from the same type of pulp but with various fiber orientations. Szilard *(26)* proposed that the shear modulus is governed by the geometric mean modulus, which was substantiated by experimental data of Baum *et al. (27)* for several different papers. Such a relationship would contradict the laminate model results, where the geometric mean modulus remains constant (Fig. 4A), while the shear modulus decreases (Fig. 4B) with increased sheet anisotropy. More experimental data are required to further investigate this issue. Poisson's ratio, ν_{LT}, was experimentally found to increase with increased fiber orientation *(27)*, but the data are for different papers, which complicates comparison with the present model.

More extensive experimental data exist on the mechanical properties for a given paper over a range of relative humidities *(27)*. We selected linerboard data of Baum *et al. (27)* for comparison because of the chemical similarity with the fibers considered in the laminate analysis. To enable comparison with the experimental data, the fibril-orientation parameters of the model were adjusted to provide a sheet that, at low-humidity conditions (20% RH), had a similar modulus ratio, E_L/E_T, as the sheet studied experimentally *(27)*. The moisture content and the modulus of the hemicellulose at any given RH can be obtained from the absorption isotherms provided by Cousins *(21)*. The elastic constants were then calculated over a range of relative humidities from zero to 80%, and these results are presented in **Table III**.

Figure 5 shows experimental *(27)* and calculated moduli E_L, E_T, and

G_{LT} over the range of relative humidities considered. To simplify comparison, the theoretical and experimental moduli were plotted in different scales (left and right, respectively) that differ by a factor of 6.67 (theoretical/experimental). The substantial difference between theoretical and experimental moduli is obviously largely a result of the continuum modeling. While the analytical results correspond to sheets with zero void content, the actual sheets examined by Baum *et al.* *(27)* contain more than 50% voids, which, as will be further discussed in Part 2 *(13)*, substantially reduces the calculated moduli. Qualitatively, however, the results are in reasonable agreement, although the experimental modulus in the MD drops faster with increased RH than the theoretically calculated modulus.

Figure 6 shows the calculated and experimental Poisson's ratio, ν_{LT}, over a range of relative humidity. As will be discussed in Part 2 *(13)*, the Poisson's ratio is less sensitive to voids than the elastic stiffnesses, which may explain the relative closeness of the results.

Figure 7 shows experimental and theoretical results for modulus ratio, E_L/E_T, over a range of relative humidity. At high relative humidities, the model predicts a larger ratio than borne out by the experiments. This is obviously the result of the model underestimating the softening influence of E_L at large relative humidities, as seen in Fig. 5.

Coefficients of hygroexpansion

The coefficients of hygroexpansion, β_T and β_L, for isotropic and oriented paper sheets were calculated from Eq. 6 at a moisture content of 9%. The results are listed in **Table IV**. It is found that with increasing fiber orientation, β_L decreases whereas β_T increases, which is in qualitative agreement with experimental data *(9)*. **Figure 8** compares the hygroexpansional ratio, β_T/β_L, with the elastic-modulus ratio, E_L/E_T. β_T/β_L is very close to E_L/E_T at low anisotropies, but the ratio deviates from the linear trend at $E_L/E_T \approx 2$. The geometric mean $(\beta_L/\beta_T)^{1/2}$ is almost constant with increased anisotropy, in agreement with experimental data *(9)*.

Table V compares the coefficients of hygroexpansion obtained by the discrete laminate model of Salmen *et al.* *(9)* and those obtained from the present model with experimental data for isotropic and oriented sheets. The laminate model of Salmen *et al.* *(9)* fairly accurately predicts the coefficient of hygroexpansion for the isotropic sheet, but it underestimates β_L and overestimates β_T for the oriented sheet. The present laminate model is in much closer agreement with the experimentally observed data for both the isotropic and oriented sheets. As will be discussed in Part 2 of this study *(13)*, voids do not influence the coefficients of hygroexpansion.

Conclusions

The composite laminate model generates baseline elastic constants and coefficients of hygroexpansion for void-free paper sheets made from chemical pulp. The model demonstrates that geometric mean modulus, $(E_LE_T)^{1/2}$, is independent of anisotropy, which is in agreement with experimental trends. However, the model shows a decrease in shear modulus with increased alignment of the fibrils in the machine direction, which appears to be in conflict with experimental data.

The influence of relative humidity on the elastic constants was calculated and compared with experimental data for linerboard *(27)*. The calculated elastic and shear moduli were much larger than the experimental values, which is largely attributed to the neglect of voids in the laminate model. These results clearly point to the need of incorporating voids in the modeling of the elastic stiffnesses of paper, which is the subject of Part 2 of this article *(13)*.

The calculated elastic moduli decreased with relative humidity. These results are qualitatively similar to the experimental data, with the exception of the Young's modulus in the machine direction, E_L, which was less sensitive to humidity than observed experimentally. The coefficients of hygroexpansion were in good agreement with experimental data by Salmen *et al.* *(9)*, and there is no need to correct hygroexpansion coefficients for the presence of voids. ▣

Literature cited

1. Steenberg, B., *Svensk Papperstid.* 50: 346(1947).
2. Cox, H. L., *British J. Appl. Phys.* 3: 72(1952).
3. Onogi, S. and Sasaguri, K., *Tappi* 44(12): 874(1961).
4. Van den Akker, J. A., "Some theoretical considerations on the mechanical properties of fibrous structures," in *Formation and Structure of Paper*, Transactions of 1961 Symposium, British Paper and Board Makers Assoc., London, 1962, pp. 205–41.
5. Kallmes, O. J., Stockel, I. H., and Bernier, G. A., *Pulp Paper Mag. Can.* 64(10): T449(1963).
6. Perkins, R. W. and Mark, R. E., *Tappi* 59(12): 118(1976).
7. Page, D. H. and Seth, R. S., *Tappi* 62(9): 99(1979); 63(6): 113(1980); 63(10): 99(1980).
8. Nissan, A. H., *Trans. Faraday Soc.* 53: 700(1957).
9. Salmen, L., Carlsson, L. A., Fellers, C., *et al.*, *Fibre Sci. Technol.* 20: 283(1984).
10. Schulgasser, K. and Page, D. H., *Composite Sci. Technol.* 32: 279(1988).
11. Gibson, L. J. and Ashby, M. F., *Cellular Solids—Structure and Properties*, Pergamon, Oxford, 1988.
12. Christensen, R. M., *J. Mech. Phys. Solids* 34(6): 563(1986).
13. Subramanian, L. and Carlsson, L. A., *Tappi J.* 77(12): (1994).
14. Tsoumis, G., *Wood as a Raw Material*, Pergamon, New York, 1968.
15. Mark, R. E., *Cell Wall Mechanics of Tracheids*, Yale University Press, New Haven, CT, 1967.
16. Page, D. H., El-Hosseiny, F., Winkler, K., *et al.*, *Tappi* 60(4): 114(1977).
17. Jones, R. M., *Mechanics of Composite Materials*, McGraw–Hill, New York, 1975.
18. Carlsson, L., *Fibre Sci. Technol.* 14: 201(1981).
19. Schulgasser, K., *J. Matl. Sci.* 20: 859(1985).

20. Sakurada, I., Nukushina, Y., and Ito, T., *J. Polymer Sci.* 57: 651(1962).
21. Cousins, W. J., *Wood Sci. Technol.* 12: 161(1978).
22. Halpin, J. C. and Kardos, J. L., *Polymer Eng. Sci.* 16(5): 344(1976).
23. Subramanian, L., "Analysis of the influence of voids on the hygroelastic properties of paper," M.S. thesis, Dept. of Mechanical Engineering, Florida Atlantic University, Boca Raton, FL, Aug. 1993.
24. Schapery, R. A., *J. Composite Matl.* 2: 380(1968).
25. Htun, M. and Fellers, C., *Tappi* 65(4): 113(1982).
26. Szilard, R., *Theory and Analysis of Plates*, Prentice–Hall, Englewood Cliffs, NJ, 1974.
27. Baum, G. A., Brennan, D. C., and Habeger, C. C., *Tappi* 64(8): 97(1981).

The authors wish to acknowledge the financial support of the TAPPI Foundation (Pe–96–93). Thanks are also due to Alf de Ruvo of SCA Research, Sweden, for providing additional support. Finally, the authors gratefully acknowledge the Dept. of Ocean Engineering at Florida Atlantic University for the use of their computational facilities.

Received for review Jan. 25, 1994.

Accepted June 22, 1994.

Research for this paper was supported through funding by the TAPPI Foundation. It is the first of many papers resulting from Foundation support that will be published in Tappi Journal. For information on the Foundation, call (404) 446-1400., ext. 266 or 211.

Appendix

Determination of the extensional stiffnesses A_{ij}

For a continuous distribution of ply orientations, extensional stiffnesses A_{ij} are given by an earlier work *(23)*.

$$A_{ij} = h \int_{-\pi/2}^{\pi/2} \overline{Q}_{ij}(\theta)\, f(\theta)\, d\theta \qquad \text{(A1)}$$

for

$i, j \quad = 1, 2, 6$

where

$h \quad$ = laminate thickness

and

$$f(\theta) = (1/\pi)(1 + a_{C,1} \cos 2\theta + a_{C,2} \cos 4\theta) \qquad \text{(A2)}$$

After substitution of $f(\theta)$ into Eq. A1:

$$A_{11} = (h/2)\,(U_1 + U_3 a_{C,2} + U_2 a_{C,1}) \qquad \text{(A3a)}$$

$$A_{12} = (h/2)\,(2U_4 - U_3 a_{C,2}) \qquad \text{(A3b)}$$

$$A_{22} = (h/2)\,(U_1 + U_3 a_{C,2} - U_2 a_{C,1}) \qquad \text{(A3c)}$$

$$A_{66} = (h/2)\,(2U_5 - U_3 a_{C,2}) \qquad \text{(A3d)}$$

where

$U_i \quad$ = lamina invariants defined by Jones *(17)* for $i = 1, 2, \ldots, 5$.

Hygroscopic forces in a paper sheet

For a laminate with a continuous distribution of ply-orientation angles, Eq. 2 yields:

$$F_L = \int_{-\pi/2}^{\pi/2} \overline{Q}_{11}(\beta_1 \cos^2\theta + \beta_2 \sin^2\theta) + \overline{Q}_{12}(\beta_1 \sin^2\theta + \beta_2 \cos^2\theta) + 2\overline{Q}_{16}(\beta_1 - \beta_2)\sin\theta\cos\theta]\; f(\theta)\, d\theta\, \Delta M \qquad \text{(A4a)}$$

$$F_T = \int_{-\pi/2}^{\pi/2} \overline{Q}_{12}(\beta_1 \cos^2\theta + \beta_2 \sin^2\theta) + \overline{Q}_{22}(\beta_1 \sin^2\theta + \beta_2 \cos^2\theta) + 2\overline{Q}_{26}(\beta_1 - \beta_2)\sin\theta\cos\theta]\; f(\theta)\, d\theta\, \Delta M \qquad \text{(A4b)}$$

$$F_{LT} = 0 \qquad \text{(A4c)}$$

After substitution of the two-parameter fibril-orientation distribution function (Eq. 8) and integration, F_L and F_T become

$$F_L = \Delta M\,(\{[(\beta_1+\beta_2)/2](A_{11}+A_{12})\} - \{[(\beta_1-\beta_2)/4][a_{C,1}(U_1+2U_3-U_4)]\} + [U_2(1+a_{C,2})]) \qquad \text{(A5a)}$$

$$F_T = \Delta M\,(\{[(\beta_1+\beta_2)/2](A_{12}+A_{22})\} - \{[(\beta_1-\beta_2)/4][a_{C,1}(U_1-U_4)]\} - [U_2(1+a_{C,2})]) \qquad \text{(A5b)}$$